INFECTION AND IMMUNITY, July 2008, p. 2978–2990 Vol. 76, No. 7
0019-9567/08/$08.00+0 doi:10.1128/IAI.00075-08

Hemolysin of Uropathogenic *Escherichia coli* Evokes Extensive Shedding of the Uroepithelium and Hemorrhage in Bladder Tissue within the First 24 Hours after Intraurethral Inoculation of Mice▽

Yarery C. Smith,[1] Susan B. Rasmussen,[1] Kerian K. Grande,[1] Richard M. Conran,[2] and Alison D. O'Brien[1]*

Department of Microbiology and Immunology[1] and Department of Pathology,[2] Uniformed Services University of the Health Sciences, 4301 Jones Bridge Road, Bethesda, Maryland 20814-4799

Received 18 January 2008/Returned for modification 24 March 2008/Accepted 22 April 2008

Many uropathogenic *Escherichia coli* (UPEC) strains produce both hemolysin (Hly) and cytotoxic necrotizing factor type 1 (CNF1), and the loci for these toxins are often linked. The conclusion that Hly and CNF1 contribute to urovirulence is supported by the results of epidemiological studies associating the severity of urinary tract infections (UTIs) with toxin production by UPEC isolates. Additionally, we previously reported that mouse bladders and rat prostates infected with UPEC strain CP9 exhibit a more profound inflammatory response than the organs from animals challenged with CP9*cnf*$_1$ and that CNF1 decreases the antimicrobial activities of polymorphonuclear leukocytes. More recently, we created an Hly mutant, CP9Δ*hlyA*$_1$::*cat*, and showed that it was less hemolytic and destructive for cultured bladder cells than CP9 was. Here we evaluated the relative effects of mutations in *hlyA*$_1$ or *cnf*$_1$ alone or together on the pathogenicity of CP9 in a mouse model of ascending UTI. To do this, we constructed an *hlyA*$_1$-complemented clone of CP9Δ*hlyA*$_1$::*cat* and an *hlyA*$_1$ *cnf*$_1$ CP9 double mutant. We found that Hly had no influence on bacterial colonization of the bladder or kidneys in single or mixed infections with the wild type and CP9Δ*hlyA*$_1$::*cat* but that it did provoke sloughing of the uroepithelium and bladder hemorrhage within the first 24 h after challenge. Finally, we confirmed that CNF1 expression induces bladder inflammation and, in particular, as shown in this study, submucosal edema. From these data, we speculate that Hly and CNF1 may be largely responsible for the signs and symptoms of cystitis in humans infected with toxigenic UPEC.

Urinary tract infections (UTIs) include infections of the bladder (cystitis) and/or kidney (pyelonephritis) and account for more than 7 million office visits each year by otherwise healthy women (23). Extraintestinal pathogenic *Escherichia coli* (ExPEC) is the causative agent of at least 80% of all uncomplicated UTIs. ExPEC strains that cause a UTI are called uropathogenic *E. coli* (UPEC). UPEC strains typically are members of phylogenetic group B2 or D and often exhibit specific O:K:H serotypes, as well as various combinations of virulence factors, including, among others, adhesins or fimbriae, siderophore systems, and toxins. The virulence-associated genes in UPEC are frequently clustered together in "pathogenicity islands" (PAIs) (25), and many UPEC isolates harbor more than one PAI. For instance, the prototypic UPEC clinical strain J96 (O4:K6) carries two PAIs, PAI I$_{J96}$ and PAI II$_{J96}$ (58). PAI I$_{J96}$ is over 170 kb long and contains operons encoding alpha-hemolysin (*hly*) and Pap fimbriae (*pap*). PAI II$_{J96}$ is 110 kb long and also contains an *hly* operon in addition to genes encoding Prs fimbriae (*prs*) and cytotoxic necrotizing factor type 1 (CNF1) (*cnf*$_1$) (6). Here, we hypothesized that the link between PAI II$_{J96}$ and the urovirulence of *E. coli* strains may largely reflect the fact that these strains produce both alpha-hemolysin (referred to as hemolysin [Hly] here) and CNF1. Indeed, epidemiological studies have consistently shown that UPEC strains that make CNF1 also produce Hly (5, 17, 19, 36, 66). Moreover, Real and coworkers reported that CNF1/Hly-expressing UPEC strains are more often isolated from humans with hemorrhagic UTIs who also have higher urinary levels of proinflammatory cytokines, such as interleukin-8 and monocyte chemoattractant protein 1, than UPEC strains that do not make these toxins (51). Landraud et al. provided a genetic explanation for the apparent linkage between CNF1 and Hly synthesis by UPEC; they demonstrated that a *cnf*$_1$ gene and an *hly* operon in the prototypic UPEC strain J96 not only are cotranscribed but also are coregulated in vitro (37).

CNF1 is a ~115-kDa cytoplasmic protein (8, 15, 16, 20) that is present in certain diarrheagenic as well as uropathogenic strains of *E. coli* (2–4, 9, 10, 45). This molecule is a member of a bacterial toxin family that modifies the function of key regulatory molecules within the Rho family of GTP-binding proteins in mammalian cells (1). Specifically, CNF1 catalyzes the deamidation of a glutamine residue at position 63 in RhoA (22, 57) and at position 61 in both Cdc42 and Rac1 (38, 39). These deamidation reactions cause constitutive activation of RhoA, Rac, and Cdc42 (i.e., they maintain these GTPases in the GTP-bound state), which in turn triggers a myriad of effects on the target cell. Specifically, activation of RhoA, Rac, and/or Cdc42 can evoke actin cytoskeleton rearrangements (27, 28, 50, 52, 53), cell cycle abnormalities (14, 21, 24), and alterations in host cell gene signaling pathways that involve certain nuclear transcription factors (39, 48). Of relevance to this study, we

* Corresponding author. Mailing address: Department of Microbiology and Immunology, Uniformed Services University of the Health Sciences, 4301 Jones Bridge Road, Bethesda, MD 20814-4799. Phone: (301) 295-3419. Fax: (301) 295-3773. E-mail: aobrien@usuhs.mil.

▽ Published ahead of print on 28 April 2008.

previously found that CNF1$^+$ UPEC strains elicit a more intense inflammatory response than isogenic CNF1$^-$ mutants elicit in a mouse model of ascending UTI (55), as well as in a rat model of prostatitis (54). We also discovered that UPEC strain CP9 survives better than a CNF1$^-$ isogenic mutant of this strain in the presence of both human (55) and mouse polymorphonuclear leukocytes (13).

Hly is a heat-labile extracellular protein made by a large proportion of ExPEC isolates (31). This toxin forms pores in the membranes and lyses a number of mammalian cell types, including red blood cells (RBCs) (hence, the name) (for reviews, see references 35 and 65). The Hly operon is comprised of, in order from the promoter, *hlyC* (which encodes a novel homodimeric lysyl-acyltransferase responsible for the fatty acid acylation step needed to render the prohemolysin active), *hlyA* (which encodes the Hly protein), *hlyB* (which encodes an integral membrane ATPase), and *hlyD* (which encodes an accessory or membrane fusion protein) (for reviews, see references 29 and 34). The acylated active Hly is exported through the outer membrane protein conduit TolC (for a review, see reference 29). The circumstantial evidence that Hly is associated with the virulence of ExPEC in general and UPEC in particular is compelling, but defining the actual role that Hly may play in pathogenicity has been elusive (40, 46, 61, 64). In a previous study, we constructed an *hlyA* mutant with a mutation in the operon located proximal to cnf_1 in strain CP9 (referred to below as $hlyA_1$ to distinguish it from $hlyA_2$ in the operon not linked to cnf_1) (61). We found that this mutation dramatically reduced the hemolytic activity of CP9, as well as its capacity to damage uroepithelial cells in tissue culture and in three-dimensional uro-organoids (61). From these results, we concluded that the hly_1 operon linked to cnf_1 conferred almost all of the hemolytic properties to CP9.

In this investigation, we sought to determine what effect the expression of Hly and CNF1, alone and in combination, has on the uropathogenicity of CP9 in mice infected intraurethrally. Therefore, we completed generation of a set of cnf_1 and $hlyA_1$ mutants by creating an $hlyA_1$-complemented clone of CP9 $\Delta hlyA_1$::*cat* and a CP9 cnf_1 $hlyA_1$ double mutant. We then used these clones and our CP9 wild-type strain and CP9cnf_1 mutant to perform a comparative evaluation of the impact of these strains on colonization and the pathology of the bladders specifically and the kidneys in a subset of animals at 1, 3, and 5 days after intraurethral infection. The results of these studies revealed, for the first time, a clear role for Hly in the induction of damage to the superficial cell layers of the murine bladder, as well as hemorrhage in the bladder tissue, but only during the first day after infection. Furthermore, we not only validated our previous observations concerning CNF1-mediated exacerbation of inflammation in UPEC-infected bladders but also extended the findings to reveal the continued impact of the toxin 5 days after intraurethral inoculation of UPEC and the striking effect of CNF1 on elicitation of submucosal edema in the bladder.

MATERIALS AND METHODS

Strains and media. The UPEC strains and plasmids used in this study are listed in Table 1. CP9 is an *E. coli* blood isolate obtained from a patient with sepsis hospitalized at the National Institutes of Health (56). This strain is of the 04/K54/H5 serotype and is characterized by its capacity to grow in 80% normal human serum, produce Hly and CNF1, and express P (class I PapG adhesin), Prs (class III PapG adhesin), and type I pili. CP9 also contains a 36.2-kb cryptic plasmid (pJEG) but does not make aerobactin. The media used in this study were Luria-Bertani (LB) broth and LB agar (Difco, Becton-Dickinson, Sparks, MD) that were supplemented, as needed, with ampicillin (100 μg/ml) or chloramphenicol (30 μg/ml).

TABLE 1. Bacterial strains and plasmids used in this study

Strain or plasmid	Relevant genotype	Reference or source
E. coli isolates		
CP9 (O4:H5:K54) (parent)	$hlyA_1^+$ $hlyA_2^+$ cnf_1^+	56
CP9cnf_1	$hlyA_1^+$ $hlyA_2^+$ cnf_1	55
CP9Δ$hlyA_1$::*cat*	$hlyA_1$ $hlyA_2^+$ cnf_1^+	61
CP9cnf_1Δ$hlyA_1$::*cat*	$hlyA_1$ $hlyA_2^+$ cnf_1	This study
CP9Δ$hlyA_1$::*cat*(pKG8)	$hlyA_1^+$ $hlyA_2^+$ cnf_1^+, pKG8	This study
CP9Δ$hlyA_1$::*cat*(pQE30)	$hlyA_1$ $hlyA_2^+$ cnf_1^+, pQE30	This study
Plasmids		
pQE30	Amp^r, low-copy-number *E. coli* expression vector	QIAGEN
pKG8	$hlyA_1$ cloned into pQE30	This study

Generation of the CP9cnf_1Δ$hlyA_1$::*cat* mutant and an $hlyA_1$-complementing clone of CP9Δ$hlyA_1$::*cat*. As mentioned above, CP9 carries two *hly* genes. The $hlyA_1$ gene is located in an operon upstream of cnf_1 (unpublished observation), as it is in other UPEC strains, such as J96 (6, 33, 37, 62). In this investigation, we introduced a nonpolar mutation in $hlyA_1$ into the isogenic CP9cnf_1 mutant strain by using the lambda red recombination technique (12), with the modifications described below. Oligonucleotides KG03F and KG04R (Table 2) were used to PCR amplify the chloramphenicol acetyltransferase gene (*cat*) sequence in pACYC184 (New England Biolabs, Ipswich, MA). Oligonucleotides KG01F and KG02R (Table 2) were designed using the previously published *hly* operon sequence of UPEC strain J96 (GenBank accession no. M10133) and were used to add sequences that flank $hlyA_1$ to the *cat* gene. The resulting 720-bp PCR product, which was generated to create a precise in-frame deletion of $hlyA_1$ and for insertion of *cat* in place of this gene (Fig. 1A), was gel purified with a Qiaex II gel extraction kit (QIAGEN, Valencia, CA) and then transformed into CP9cnf_1 by electroporation at 2.5 V, 200 Ω, and 25 μF. Hly mutants were selected on medium with 30 μg/ml chloramphenicol and screened for acquisition of the *cat* gene by PCR (primers KG03F and KG04R [Table 2]), and then colonies of the mutant were evaluated on tryptic soy agar with 5% ovine blood (Remel Inc., Lenexa, KS) for reduced hemolysis. Insertion of *cat* into the $hlyA_1$ locus was verified by amplification of PCR products with primers that extended from within *cat* downstream (KG03F and KG08R [Table 2]) or upstream (KG07F and KG04R [Table 2]) into the $hlyA_1$-flanking regions. Primers specific for the regions flanking $hlyA_1$ (KG07F and KG08R [Table 2]) were used to confirm replacement of the 3.1-kb $hlyA_1$ gene with the 660-bp *cat* gene.

A Southern blot analysis (ECL direct nucleic acid labeling and detection system; Amersham Biosciences, Piscataway, NJ) of NcoI-digested chromosomal DNA (predicted digests [Fig. 1A]) from the CP9cnf_1 $hlyA_1$ mutant compared to the chromosomal DNA of CP9cnf_1 was performed (Fig. 1B). As anticipated, the cnf_1 band was evident in the blot for wild-type strain CP9 and the CP9 $hlyA_1$ mutant (Fig. 1B, lanes 1 and 3, respectively) but not in the blot for either CP9cnf_1 (Fig. 1B, lane 2) or the cnf_1 $hlyA_1$ double mutant (Fig. 1B, lane 4). A probe specific for the $hlyA_1$ fragment upstream of an internal NcoI site was PCR amplified (KG12F and KG13R [Table 2]). The two native *hlyA* genes were found on NcoI fragments that were approximately 7 and 8 kb long in the wild-type chromosomal digest and the cnf_1 mutant (Fig. 1C, lanes 1 and 2, respectively). The cnf_1-linked $hlyA_1$ gene was not present in either the CP9Δ$hlyA_1$::*cat* mutant (Fig. 1C, lane 3), as previously reported (61), or the newly constructed CP9cnf_1Δ$hlyA_1$::*cat* mutant (Fig. 1C, lane 4). The location of the $hlyA_1$ mutation in the *hly* operon adjacent to the cnf_1 locus was confirmed by performing long-range PCR with *Pfu* TURBO (Stratagene, La Jolla, CA) and the following primer sets: KG03F-KG10R and KG09F-KG10R (Fig. 2A).

The CP9cnf_1Δ$hlyA_1$::*cat* mutant grew at wild-type levels and exhibited a reduced hemolytic phenotype on blood agar plates compared to CP9 (not shown). As expected, the cnf_1 $hlyA_1$ double mutant did not produce CNF1, as shown by Western blot analysis (Fig. 2B) and HEp-2 cell multinucleation assays of equal

TABLE 2. Oligonucleotide primers

Primer[a]	Sequence	Target	Reference
KG01F	5′-CAGATTTCAATTTTTCATTAACAGGTTAAGAGGTAA TTAAATGGAGAAAAAAATCACTGG-3′	40 bp upstream of $hlyA_1$ and first 20 bp of *cat*	61
KG02R	5′-CAGCCCAGTAAGATTGCTATTATTTAAATTAATAAA TTACGCCCCGCCCTGCC-3′	5′ last 33 bp of *cat* and 20 bp downstream of $hlyA_1$	61
KG03F	5′-ATGGAGAAAAAAATCACTGG-3′	*cat*	61
KG04R	5′-TTACGCCCCGCCCTGCC-3′	*cat*	61
KG07F	5′-CCATTAGAGGTTCTTGGGC-3′	Upstream of $hlyA_1$	61
KG08R	5′-GGAATAAACCAGGTAAAGTC-3′	Downstream of $hlyA_1$	61
KG09F	5′-ATACTGTATCGGGTATTTTATC-3′	$hlyA_1$	61
KG09R	5′-TATGGTCATCACCATCCGC-3′	$hlyA_1$	This study
KG10R	5′-GATACCAACTCATTGTACTCA-3′	cnf_1	61
KG11F	5′-GATTAATGGTGATACTTATGAAG-3′	cnf_1	This study
KG11R	5′-GCCATGGTTATCAAAGCGATC-3′	cnf_1	This study
KG12F	5′-ATACTGTATCGGGTATTTTATC-3′	Upstream of NcoI site, $hlyA_1$	This study
KG13R	5′-TATGGTCATCACCATCCGC-3′	Upstream of NcoI site, $hlyA_1$	This study

[a] F, forward; R, reverse.

concentrations of sonicated cellular protein (data not shown) (Fig. 2B, lanes 1, 2, and 3, have been shown previously [61] and are included for comparison with lane 4 [cnf_1 $hlyA_1$ double mutant]). Protein concentrations were determined by using the methods described for a BCA protein assay kit from Pierce (Rockford, IL). Western blot analysis was done as described elsewhere with goat polyclonal anti-CNF1 serum as the probe (44).

A complementing clone of the CP9Δ$hlyA_1$::*cat* mutant was constructed as follows. The $hlyA_1$ gene was amplified by PCR from the chromosome of UPEC

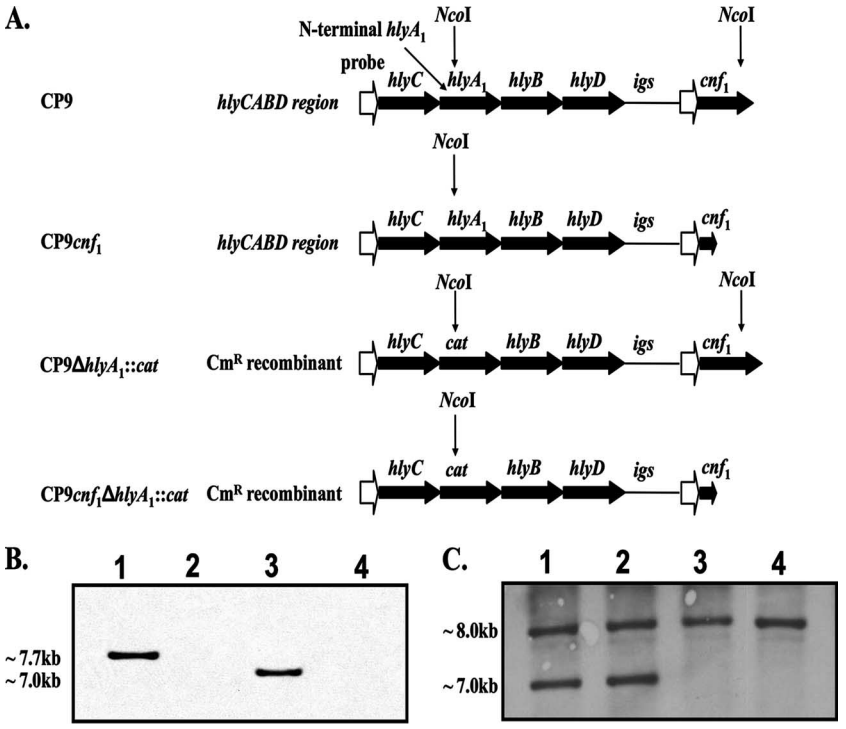

FIG. 1. Diagram of the CP9 *hly* operon upstream of cnf_1 and Southern blot analyses. (A) The mutated or wild-type Hly operon, the intergenic sequence (*igs*), and the cnf_1 gene from the chromosome of strains CP9, CP9cnf_1, CP9Δ$hlyA_1$::*cat*, and CP9cnf_1Δ$hlyA_1$::*cat* are indicated by large filled arrows. Promoter regions (open arrows) are also shown. Sites of NcoI cleavage (indicated by vertical arrows) of chromosomal DNA were predicted from database sequences (J96 *hly* operon, GenBank accession no. M10133; cnf_1, GenBank accession no. X70670; pACYC184 *cat* gene, GenBank accession no. X06403; J96 *igs*, GenBank accession no. X70670). (B) Southern blot to detect the NcoI-NcoI cnf_1 fragment. Lane 1, CP9; lane 2, CP9cnf_1; lane 3, CP9Δ$hlyA_1$::*cat*; lane 4, CP9cnf_1Δ$hlyA_1$::*cat*. As expected, the fragment of the chromosome that contained the cnf_1 gene was discernible in strains CP9 and CP9Δ$hlyA_1$::*cat* (lanes 1 and 3, respectively). The cnf_1-specific band size (~7.7 kb) was reduced (~7.0 kb) in the CP9Δ$hlyA_1$::*cat* strain because $hlyA_1$ was replaced by the smaller *cat* gene. A cnf_1-specific band was absent in the cnf_1 mutants (lanes 2 and 4) because the cnf_1 probe (KG11F and KG11R) binds to a region of cnf_1 that is absent in the mutant strains (due to internal deletion of a 1.2-kb BclI fragment). (C) Southern blot to detect the NcoI-NcoI *hlyA* fragment(s). Lane 1, CP9; lane 2, CP9cnf_1; lane 3, CP9Δ$hlyA_1$::*cat*; lane 4, CP9cnf_1Δ$hlyA_1$::*cat*. As anticipated, two copies of *hlyA* were evident in strains CP9 and CP9cnf_1 (lanes 1 and 2, respectively), but only one band was apparent in the $hlyA_1$ mutants (lanes 3 and 4) due to deletion of one *hlyA* gene locus.

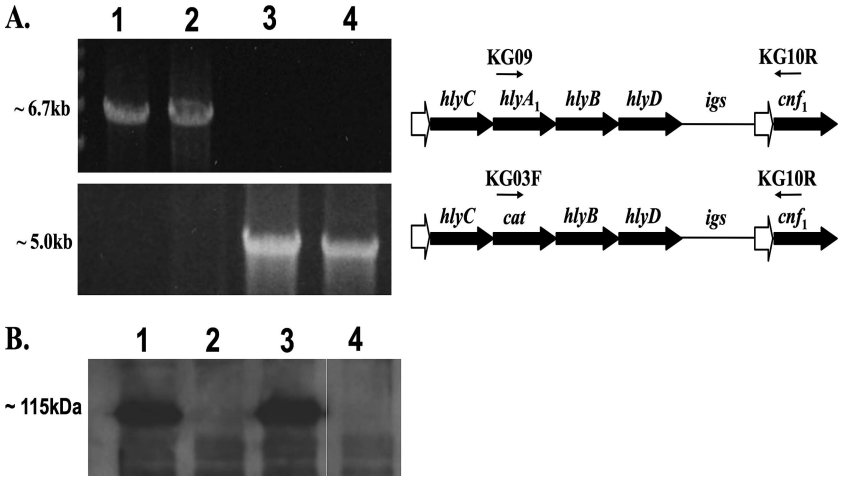

FIG. 2. Long-range PCR. (A) Primers KG09 and KG10R (arrows above the hemolysin operon) were used to test for the presence of an *hlyA*$_1$-containing PCR fragment amplified from *hlyA*$_1$ to the *cnf*$_1$ gene on the chromosome of the following strains: CP9 (lane 1), CP9*cnf*$_1$ (lane 2), CP9Δ*hlyA*$_1$::*cat* (lane 3), and CP9*cnf*$_1$Δ*hlyA*$_1$::*cat* (lane 4). PCR products (~6.7 kb) were present for CP9 and CP9*cnf*$_1$ but not for CP9Δ*hlyA*$_1$::*cat* and CP9*cnf*$_1$Δ*hlyA*$_1$::*cat*, as shown in the top panel of the ethidium bromide-stained agarose gel on the left. Primers KG03F and KG10R were used to verify the replacement of *hlyA*$_1$ with *cat* upstream of the *cnf*$_1$ gene in mutant strains CP9Δ*hlyA*$_1$::*cat* and CP9*cnf*$_1$Δ*hlyA*$_1$::*cat* (~5.0-kb amplified PCR product from *cat* to *cnf*$_1$ in the bottom panel of the ethidium bromide-stained agarose gel). (B) Western blot analysis with polyclonal anti-CNF1 serum as a probe was used to verify that wild-type levels of CNF1 (lane 1) were produced by CP9Δ*hlyA*$_1$::*cat* (lane 3) and that, as expected, strains CP9*cnf*$_1$ and CP9*cnf*$_1$Δ*hlyA*$_1$::*cat* did not produce CNF1 (lanes 2 and 4, respectively).

strain CP9 and then ligated into pQE30 (QIAGEN, Valencia, CA) at the KpnI and BamHI enzyme sites. The clone was confirmed by restriction analysis and PCR with primers for the *hlyA*$_1$ gene (KG09F and KG09R). The resulting plasmid, pKG8, was transformed into CP9Δ*hlyA*$_1$::*cat* by electroporation and selected by plating preparations on LB agar that contained ampicillin. That complementation had occurred was evident from the zones of hemolysis surrounding colonies of CP9Δ*hlyA*$_1$::*cat*(pKG8) on blood agar plates supplemented with ampicillin that were larger than the zones that were observed around colonies of the mutant CP9Δ*hlyA*$_1$::*cat* (Fig. 3) or colonies of a strain transformed with the cloning vector pQE30 (not shown). On average, the hemolytic halos around CP9Δ*hlyA*$_1$::*cat*(pKG8) colonies appeared to be smaller than those surrounding CP9 (Fig. 3), an observation that indicates that the mutant was complemented at less-than-wild-type levels.

Mouse UTI model. The ascending UTI mouse model was used essentially as previously described (26, 55), with the modifications summarized below. The bacterial inocula used for infection of mice were prepared by culturing the strains in static LB broth for 48 h at 37°C, growth conditions that have been reported to enhance expression of type 1 pili (47). The extent of type 1 pilus expression was confirmed by mannose-sensitive agglutination of 1% baker's yeast suspended in Dulbecco's phosphate-buffered saline (PBS) (Cambrex BioSciences/Lonza, Walkersville, MD) (41, 42). The bacterial concentration was then adjusted to an A_{600} of ~0.85, and 6 ml of each suspension was pelleted by centrifugation (10,000 × *g* for 5 min at 4°C) and resuspended in 0.5 ml of sterile saline (Baxter Healthcare Corporation, Deerfield, IL) to obtain a bacterial density of 10^9 CFU/ml. Each inoculum was pipetted into an adapter tube (6 in.) with a male/female line (Edwards Lifesciences, Irvine, CA) connected to a 30-gauge sterile needle (Becton Dickinson & Co, Franklin Lakes, NJ).

Four- to six-week-old C3H/HeOuJ female mice (Jackson Laboratory, Bar Harbor, ME) were used in these experiments because we and other workers (11) have previously found that this lipopolysaccharide-responsive strain of mice is readily infected by UPEC strains (55). Animals were quarantined for at least 1 week after receipt and were allowed access to water and food ad libitum. Animals were not given antibiotics to prevent loss of the *hlyA*$_1$ complementing plasmid from strain CP9Δ*hlyA*$_1$::*cat*(pKG8). The reason for this omission was that in preliminary experiments with antibiotic-free mice, the pKG8 plasmid was retained in the bacterial strain, as ascertained by comparison of colony counts of homogenates of CP9Δ*hlyA*$_1$::*cat*(pKG8)-infected bladders on LB agar with and without ampicillin.

Mice were anesthetized with isoflurane (Hospira, Inc., Lake Forest, IL), and a 1-in. (2.5-cm) sterile polyethylene catheter (inside diameter, 0.28 mm; outside diameter, 0.61 mm; Intramedic, Becton Dickinson, Sparks, MD) was inserted intraurethrally into each animal. Prior to infection, a urine sample was collected

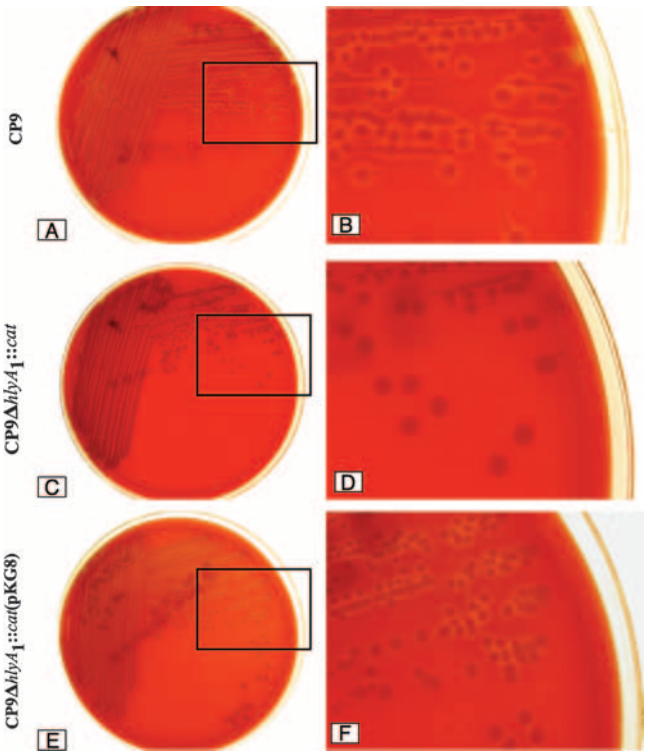

FIG. 3. Blood agar plate assay for hemolytic activity. (A) CP9 plate. (B) Enlargement of the section indicated by a box on the CP9 plate. (C) CP9Δ*hlyA*$_1$::*cat* plate. (D) Enlargement of the section indicated by a box on the CP9Δ*hlyA*$_1$::*cat* plate. (E) CP9Δ*hlyA*$_1$::*cat*(pKG8) plate. (F) Enlargement of the section indicated by a box on the CP9 Δ*hlyA*$_1$::*cat*(pKG8) plate. Strains were streaked on plates, incubated overnight at 37°C, and photographed digitally with a Nikon Coolpix 995 camera.

from each mouse to test for preexisting bacteriuria, and mice in which the bacterial levels were $>10^2$ cells/ml were excluded from the study. The needle fitted to the inoculating apparatus was inserted into the catheter, and 25 μl of each inoculum (2.5×10^7 CFU) was delivered over a 20-s period into the bladder of an anesthetized animal. Immediately after inoculation, the catheter was withdrawn from the mouse, and no further manipulations were carried out until completion of the study. At 1, 3, or 5 days postchallenge, urine was collected by catheterization, serially diluted in PBS, and plated on LB agar to determine the bacterial load. Mice were then euthanized in groups of 10 by using an isoflurane overdose. Kidneys and bladders were aseptically removed, homogenized in PBS, and serially diluted for viable counting, and the number of bacteria was expressed as the number of CFU per bladder or per kidney. Alternatively, some of the samples were prepared for histological examination. Control animals were instilled with PBS. In each experiment, at least one mouse was sacrificed immediately after inoculation, and the kidneys were aseptically removed for assessment of quantitative vesicoureteral reflux (32). All animal experiments were performed in accordance with the principles outlined in the *Guide for the Care and Use of Laboratory Animals* (49).

Histopathology. The bladder and kidneys from selected euthanized infected and control mice were removed and immediately placed in 5% phosphate-buffered formalin (Fisher Scientific, Pittsburgh, PA) for at least 12 h. The resulting formalin-fixed tissues were then embedded in paraffin and cut into 5-μm sections (Histoserv, Rockville, MD), and the resulting slides were stained with hematoxylin and eosin or with Giemsa stain for better visualization of bacteria. Four stained sections per organ per animal were prescreened, and then single organ sections were graded in a blinded manner by one of us (R. Conran, a pathologist) for each of the following histopathologic parameters: interstitial edema, hemorrhage, leukocyte infiltration, and uroepithelial destruction. A semiquantitative severity scale (0 to 5 for each parameter) was used for these evaluations. For each of the four categories assessed, average scores (for five samples) of less than 1 were considered a mild effect; scores of 2 to 3 were classified as a moderate effect, and scores greater than 4 were categorized as a severe effect of the strain on the histopathological feature.

In vitro alpha-hemolytic activity determination. Overnight cultures of CP9 or CP9Δ*hlyA*$_1$::*cat* were diluted 1:100 with LB broth (optical density at 600 nm, ~0.03) and incubated at 37°C (considered time zero). One-milliliter samples were taken hourly from time zero to 48 h, and the bacterial cells were pelleted by centrifugation (13,000 rpm, 10 min). The pellets were washed once with PBS and resuspended in 1 ml PBS. Three hundred microliters of each pellet or supernatant was mixed with 300 μl of 4% sheep RBCs (Hemostat Laboratories, Dixon, CA). Each sample was then incubated at 37°C for 1 h, and the cells were pelleted by centrifugation (13,000 rpm, 5 min). Two hundred microliters of each resultant supernatant was carefully transferred into an untreated flat-bottom 96-well microtiter plate (Corning Incorporated, Corning, NY) and read at 405 nm (A_{405}) using a plate reader (Bio-Tek Instruments, Winooski, VT). RBCs mixed with water were used as a positive control, while RBCs with PBS or LB medium served as negative controls. Images of the microtiter assay plates were obtained, and the intensity of the red color in a well correlated with the A_{405} measurement. Samples were tested for alpha-hemolytic activity no more than 5 h after the time of collection, and each determination was done in triplicate.

Western blotting. Bacterial pellets were obtained as described above for the hemolysis assay. A Western analysis was carried out essentially as previously described (43), with the following modifications. Pellets were concentrated twofold by resuspension in 0.5 ml PBS and then disrupted by sonication. Bacterial extracts were then clarified by centrifugation. The protein concentrations of clarified toxin extracts were determined by absorbance at 280 nm utilizing a NanoDrop 1000 spectrophotometer (Nanodrop Technologies LLC, Wilmington, DE), and the concentration of each extract was adjusted to 1 mg/ml. The CP9 or CP9Δ*hlyA*$_1$::*cat* pellet lysates were then subjected to sodium dodecyl sulfate-polyacrylamide gel electrophoresis (4 to 20% Tris-glycine gel; Invitrogen, Carlsbad, CA). After electrophoretic separation, the proteins were transferred to Optitran nitrocellulose membranes with a Trans-Blot SD semidry electrophoretic transfer cell (Bio-Rad), and the membranes were then blocked overnight in 5% dry milk in PBS-0.1% Tween 20. Membranes were incubated with polyclonal goat anti-CNF sera (1:10,000) (44), washed in PBS-0.1% Tween 20, and then incubated with horseradish peroxidase-conjugated porcine anti-goat sera (1:10,000) (Roche). Reactive proteins were detected by enhanced chemiluminescence (GE HealthCare, Buckinghamshire, United Kingdom).

HEp-2 cell multinucleation assay. HEp-2 multinucleation assays were performed as previously described (44), with the following modifications. Cells were seeded at a concentration of 5×10^4 cells well^{-1} into 96-well plates (Costar) and incubated for 4 h at 37°C with 5% CO_2. Dilutions (1:5) of clarified sonic lysates from bacterial cells harvested at 2 to 48 h (see above) were applied to HEp-2 cells at a starting concentration of 20 μg per well. Cells were incubated for 72 h at 37°C in the presence of 5% CO_2, fixed, and stained with Hema-3 (Fisher Scientific), and the degree of multinucleation was determined by light microscopy.

Immunofluorescence. Five-micrometer sections of infected or uninfected murine bladders were immunostained to determine the presence of uroplakin or *E. coli* as previously described (61). Briefly, fixed tissue sections were deparaffinized and then heated in a microwave oven to optimize antigen retrieval. Next, nonspecific binding sites on the treated sections were blocked with 1% bovine serum albumin (Sigma, St. Louis, MO) and then incubated for 1 h at room temperature with the appropriate primary antibody, either goat anti-uroplakin III antibody (Santa Cruz Biotechnology, Santa Cruz, CA) or rabbit anti-*E. coli* antibody (Biodesign, Saco, ME). The dilution used for each antibody was selected based on the manufacturer's recommendation. The slides were subsequently incubated for 1 h at room temperature with AlexaFluor 488- or 555-conjugated secondary antibody (Molecular Probes, Eugene OR) and mounted with Fluoromount-G (Southern Biotechnologies Associates, Inc., Birmingham, AL). All samples were analyzed with an Olympus BX60 microscope with a BX-FLA reflected-light fluorescence attachment. Images were acquired with a SPOT RT charge-coupled device digital camera (Diagnostic Instrument, Inc., Miami, FL) and assembled for presentation using Adobe Photoshop.

Statistical analysis. One-way analysis of variance (ANOVA) was used to identify statistically significant differences in the geometric mean numbers of CFU/ml of bacteria among the groups of mice. When experiments were done in triplicate, two-way ANOVA was used after adjustment for differences among experiments. Separate ANOVA analyses were done for urine, bladder, and kidney data for the different groups of mice. Statistical significance for histopathological analyses was also determined by one-way ANOVA, followed by Tukey's post hoc pairwise comparisons across the set of strains used in this investigation. P values less than 0.05 were considered statistically significant.

RESULTS

CP9 colonization versus CP9Δ*hlyA*$_1$::*cat* colonization in single- and mixed-strain infection studies over time. The overall objective of these experiments was to assess the relative importance of Hly and CNF1 individually and together in the urovirulence of UPEC strain CP9. We began our investigation by evaluating the importance of Hly in colonization because we previously tested the impact of a mutation in *cnf*$_1$ on bacterial colonization and histopathology in a mouse UTI model (55) and in a rat acute prostatitis system (54). As noted above, these previous studies revealed a significant role for CNF1 in the acute inflammation of the mouse bladder (55) and rat prostate (54), but the investigations did not reveal a statistically significant effect of CNF1 on bacterial persistence in the mouse UTI model or the rat prostrate after single-strain challenge. However, in mixed infections with wild-type strain CP9 and CP9*cnf*$_1$, CP9 outcompeted the mutant through day 9 of infection in the urine and in the bladder and kidney tissues of C3H/HeOuJ mice (55). In contrast, the growth advantage of CP9 over CP9*cnf*$_1$ was not evident in rat prostates (54). Here, we inoculated groups of 30 mice with CP9 or CP9Δ*hlyA*$_1$::*cat* intraurethrally using 2.5×10^7 CFU and then euthanized groups of 10 animals/strain at days 1, 3, and 5 postinfection. Bacterial counts in the urine and in bladder and kidney homogenates were obtained for five mice; kidneys and bladders from the other five animals were prepared for histological evaluation. The experiment was done three times. As shown in Fig. 4, no statistically significant differences in colony counts were observed in the urine, bladder, or kidneys of CP9-infected mice and CP9Δ*hlyA*$_1$::*cat*-infected mice.

Next, we asked whether coinoculation of CP9 and CP9Δ*hlyA*$_1$::*cat* would permit us to discern differences in fitness between these strains that were not apparent in the single-strain animal challenge studies described above. For this pur-

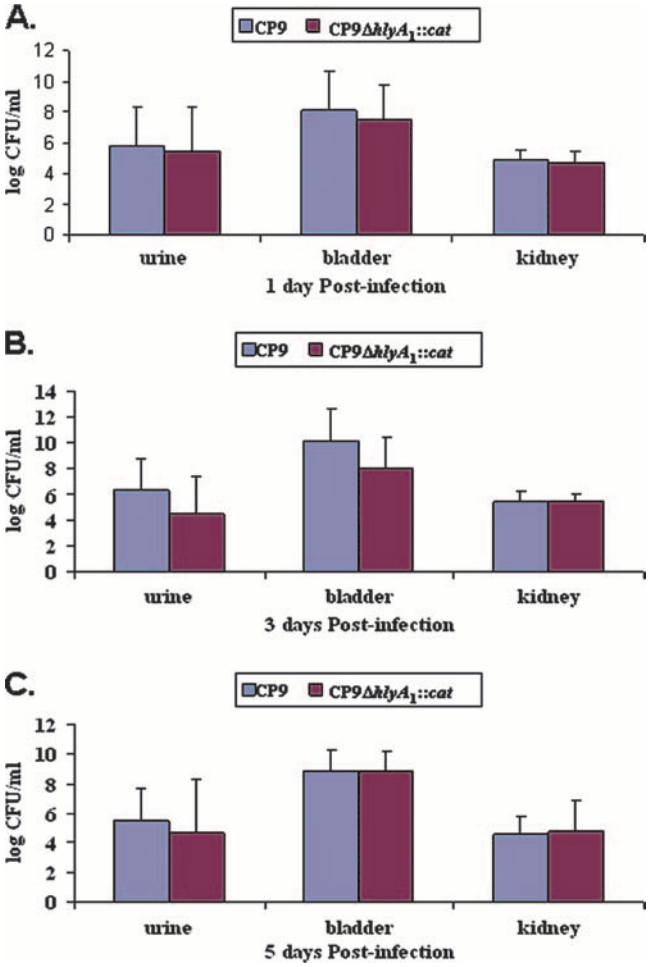

FIG. 4. Kinetics of UTI of C3H/HeOuJ mice with CP9 and the CP9Δ*hlyA*$_1$::*cat* isogenic mutant. Fifteen female C3H/HeOuJ mice were inoculated via the urethra with 2.5×10^7 CFU of either CP9 or CP9Δ*hlyA*$_1$::*cat*. After 1, 3, and 5 days, mice were euthanized and urine samples, as well as bladders and kidneys, were collected, homogenized, and plated on LB agar for bacterial enumeration. (A) Log CFU/ml for 1 day postinfection. (B) Log CFU/ml for 3 days postinfection. (C) Log CFU/ml for 5 days postinfection. Each bar indicates the geometric mean for a sample, and the error bars indicate one standard deviation above the geometric mean.

pose, we introduced equal numbers of CFU/ml of the parent CP9 strain and the *hlyA*$_1$ mutant intraurethrally into C3H/HeOuJ female mice as described in Material and Methods. Urine and bladders from the challenged animals were collected at 1 and 3 days postinfection, and colonies of the strains in the mixture were distinguished by using the chloramphenicol resistance of the *hlyA*$_1$ mutant on antibiotic-supplemented LB agar. We found that the CP9Δ*hlyA*$_1$::*cat* counts were comparable to the strain CP9 counts when the organisms were coinoculated and were at the levels observed in the single-strain UTI model (Table 3 and data not shown). One caveat to interpretation of the results of these mixed-infection studies is that it is conceivable that the Hly made by the wild-type strain could have complemented, and hence obscured, a defect in the fitness of the mutant. Nevertheless, these results, together with the results of the single-strain challenge experiments, strongly indicate that expression of Hly does not influence the extent of UPEC strain CP9 colonization.

Infection with *hlyA*$_1$-complemented CP9Δ*hlyA*$_1$::*cat* mutant. To further define any possible role that Hly may play in the pathogenesis of UPEC-mediated UTI, a CP9Δ*hlyA*$_1$::*cat* complemented mutant, CP9Δ*hlyA*$_1$::*cat*(pKG8), was created by subcloning the *hlyA*$_1$ gene into the pQE30 vector. To ensure that pQE30, the plasmid (Table 1) used for this complementation, was not itself the cause of the increase in the hemolytic effect or any other unwanted effects, we transformed the cloning vector alone into CP9Δ*hlyA*$_1$::*cat*. The growth curves for CP9Δ*hlyA*$_1$::*cat*, CP9Δ*hlyA*$_1$::*cat*(pKG8), and CP9Δ*hlyA*$_1$::*cat*(pQE30) in LB media were similar (data not shown). When we tested CP9Δ*hlyA*$_1$::*cat*(pKG8) and CP9Δ*hlyA*$_1$::*cat*(pQE30) in the mouse model of UTI, we observed no statistically significant differences in bacterial counts in the urine samples or the infected bladder homogenates at 1 day postinfection for the mice given the different strains (Table 3). Moreover, the numbers of CFU/ml in the urine or bladder tissues were similar to those seen 1 day after challenge with strain CP9 or CP9 Δ*hlyA*$_1$::*cat* (Fig. 4 and Table 3).

Bacterial colonization of the bladder by CP9*cnf*$_1$Δ*hlyA*$_1$::*cat* and CP9*cnf*$_1$. Since our primary goal was to investigate the relative contributions of CNF1 and Hly in the urovirulence of UPEC strain CP9, we examined the impact of a *cnf*$_1$ *hlyA*$_1$ double mutant on colony counts in the urine and bladders of C3H/HeOuJ mice 1 day after challenge. As a control, we included a set of mice inoculated with the previously examined CP9*cnf*$_1$ isogenic mutant (55). We observed no statistically significant differences in colony counts in the urine or bladder homogenates of animals infected with CP9*cnf*$_1$Δ*hlyA*$_1$::*cat* and animals infected with the CP9*cnf*$_1$ mutant; moreover, the numbers were similar to those for the wild type at 1 day after challenge (Table 3). In aggregate, these findings suggest that virulence factors of UPEC strain CP9 other than Hly and CNF1 are integral for bacterial colonization of the bladder, at least as evaluated at 1 day after infection (we did not test all strains after 3 and 5 days).

Histological examination of bladders. Next, we evaluated the relative impact of Hly and CNF1 on acute inflammation and damage using bladder sections from mice infected with each of the members of the CP9 isogenic strain set. We used a scoring system for coded sections that ranged from 0 to 5 for each of the following histopathological parameters: interstitial edema, hemorrhage, leukocyte infiltration, and uroepithelial

TABLE 3. Quantitative culture of CP9 UPEC strains in C3H/HeOuJ mouse samples collected 1 day postchallenge

Strain	*n*	Mean $\log_{10}$ CFU/ml (SD)[a]	
		Urine	Bladder
CP9 (O4:H5:K54) (parent)	15	5.81 (2.51)	8.12 (2.54)
CP9Δ*hlyA*$_1$::*cat*	15	5.42 (2.91)	7.42 (2.37)
CP9*cnf*$_1$	10	5.77 (2.09)	7.13 (1.32)
CP9*cnf*$_1$Δ*hlyA*$_1$::*cat*	10	5.75 (2.22)	7.33 (0.34)
CP9Δ*hlyA*$_1$::*cat*(pKG8)	10	6.43 (2.57)	8.98 (1.29)
CP9Δ*hlyA*$_1$::*cat*(pQE30)	10	5.51 (2.41)	7.59 (0.73)

[a] There were no statistically significant differences among urine counts or among bladder counts as assessed by ANOVA.

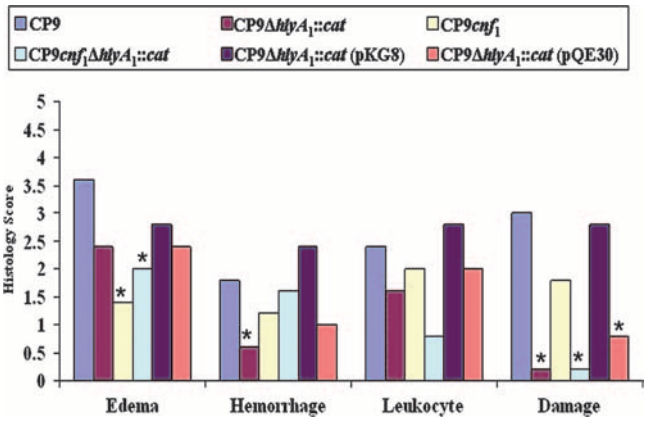

FIG. 5. Effect of CP9 strains on the histology of murine bladders. Groups of five female C3H/HeOuJ mice were inoculated via the urethra with 2.5×10^7 CFU of CP9, CP9Δ*hlyA*$_1$::*cat*, CP9*cnf*$_1$, CP9*cnf*$_1$Δ*hlyA*$_1$::*cat*, CP9Δ*hlyA*$_1$::*cat*(pKG8), or CP9Δ*hlyA*$_1$::*cat*(pQE30) and euthanized 1 day later. Bladders were removed, fixed in formalin, and processed for histological examination. Each sample was examined by light microscopy. A score of 0 to 5 was assigned to each bladder for edema, hemorrhage, leukocyte presence, and urothelial damage. Scores for each group of mice were combined, and the averages are indicated by the bars. An asterisk indicates that the tissue response to a strain was statistically significantly different from the response to the strain for which the response was greatest for the specific effect, as determined by ANOVA assessment followed by Tukey's post hoc pairwise comparisons.

destruction. The pathologist evaluator of the slides was blinded to the bacterial strain used to infect the animal from which the bladder section slides were prepared. Five tissue blocks (one block per animal) for 1 day after infection with CP9 or each CP9-derived strain were analyzed. Additional sections from bladders and kidneys harvested 3 and 5 days after infection with CP9 or CP9Δ*hlyA*$_1$::*cat* were also examined.

We found that bladders from CP9-challenged animals exhibited the highest levels of interstitial edema among the mice tested in this study (Fig. 5). The higher level of edema was evident on a representative slide taken from the tissue set scored (Fig. 6A). The fact that the interstitial edema was greatest for the parental CP9 strain and was statistically significantly different from the levels of the edema observed with the isogenic mutants CP9*cnf*$_1$ and CP9*cnf*$_1$Δ*hlyA*$_1$::*cat* (Fig. 5) ($P < 0.001$ and $P < 0.028$, respectively) indicates that the submucosal swelling was largely due to CNF1 (Fig. 6, compare panels E and I with panel A). Additionally, CP9-provoked submucosal edema remained clearly apparent at day 3 after infection (Fig. 7, compare panel A with control panel E) and was still evident at day 5 (Fig. 7C).

We also examined the extent of hemorrhage in the bladders caused by the strains used in these experiments. We found that loss of Hly, as exemplified by bladders from mice inoculated with CP9Δ*hlyA*$_1$::*cat*, resulted in the largest decrease in the degree of hemorrhage in tissues ($P < 0.041$) (Fig. 5). When we assessed the slides obtained for sections of bladders infected with the various strains for the extent of leukocyte infiltration (Fig. 5), we noted that the tissue sections from mice inoculated with CP9 and the equivalent strain CP9Δ*hlyA*$_1$::*cat*(pKG8) showed a higher influx of white cells than the tissue sections from mice inoculated with any of the other isogenic mutants. In particular, the differences were most apparent when we compared the CP9 and CP9Δ*hlyA*$_1$::*cat*(pKG8) strains to the CP9*cnf*$_1$Δ*hlyA*$_1$::*cat* mutant, although the differences were not statistically significant ($P < 0.278$ and $P < 0.104$, respectively) (Fig. 5). Furthermore, histopathological examination also revealed significantly greater damage to the urothelium in the bladders of mice infected with CP9 than in the bladders of mice infected with the CP9Δ*hlyA*$_1$::*cat* and CP9*cnf*$_1$Δ*hlyA*$_1$::*cat* mutants ($P < 0.0001$ for each strain) (Fig. 5 and Fig. 6, compare panel B with panels D and J). Additionally, we evaluated bladder sections from mice infected with the *hlyA*$_1$-complemented CP9Δ*hlyA*$_1$::*cat* mutant and the isogenic CP9Δ*hlyA*$_1$::*cat*(pQE30) mutant for uroepithelial damage at 1 day postinfection. We observed that after reinstatement of the capacity of the *hlyA*$_1$ mutant to produce Hly (Fig. 3), the complemented mutant could cause extensive uroepithelial damage (Fig. 6G and H). In contrast, markedly less destruction of the luminal surface of the bladders of mice infected with the isogenic CP9Δ*hlyA*$_1$::*cat*(pQE30) mutant was detectable (data not shown) (the appearance of sections was similar to the appearance of sections in Fig. 6C and D). Moreover, all three strains that did not make Hly [CP9Δ*hlyA*$_1$::*cat*, CP9*cnf*$_1$Δ*hlyA*$_1$::*cat*, and CP9Δ*hlyA*$_1$::*cat*(pQE30)] caused statistically significantly lower levels of damage to the murine urothelium than the strains that produced Hly [CP9, CP9*cnf*$_1$, and CP9Δ*hlyA*$_1$::*cat*(pKG8)] (Fig. 5). Overall, these in vivo results are in agreement with our previous in vitro observations which showed that a mutation in the *hlyA*$_1$ gene of strain CP9 resulted in attenuation of the uroepithelial damage that was evident soon after CP9 infection of 5637 bladder cells grown as monolayers or as three-dimensional organoids (61).

Surprisingly, at 3 days postinfection, our histopathologic observations of the murine bladders revealed no apparent urothelium injury in CP9-infected bladders (Fig. 7A and B). In fact, when we evaluated the slides containing bladder sections from mice infected with CP9 and mice infected with CP9 Δ*hlyA*$_1$::*cat* at 3 and 5 days postinfection, the uroepithelia in all sections appeared to be smooth and generally intact and much like that of the PBS-inoculated control (Fig. 7; data not shown for CP9Δ*hlyA*$_1$::*cat*-infected sections). We concluded from analyses of the day 1, 3, and 5 sections that Hly-mediated effects on the bladder appeared to be limited to the first day of infection, whereas edema, largely attributable to CNF1, at least after 1 day of infection (Fig. 5), remained readily discernible at day 3 after challenge and was still apparent at day 5 postinoculation (Fig. 7).

Alpha-hemolytic activity and CNF1 expression. We next asked whether the differences in timing of the impact of Hly and CNF1 on infected murine bladders reflected variations in the kinetics of activity of these toxins in vitro. We observed that the CP9 alpha-hemolytic activity in culture supernatants, as determined by lysis of sheep RBCs, began at 2 h, remained constant until approximately 19 to 20 h, when it started to decrease, and then decreased to background levels by 22 h postinoculation (Fig. 8A). As expected, the CP9Δ*hlyA*$_1$::*cat* mutant displayed little alpha-hemolytic activity throughout the assay (Fig. 8A). Furthermore, no alpha-hemolytic activity was seen in the PBS-resuspended pellets of the CP9 strain or its *hly* isogenic mutant at any time (data not shown). In contrast, CNF1 was detectable even at time zero and remained evident

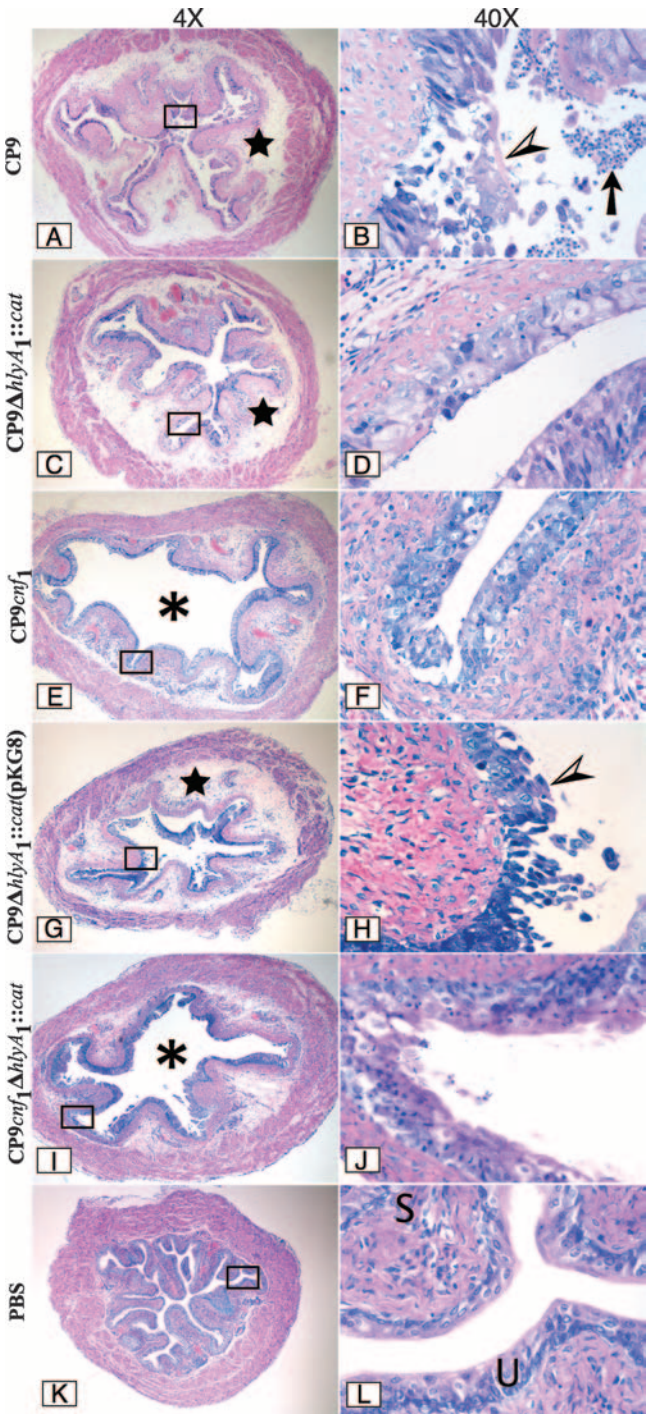

FIG. 6. Infection of female C3H/HeOuJ mice with CP9 UPEC strains. Mice were inoculated with CP9 (A and B), CP9Δ*hlyA*$_1$::*cat* (C and D), CP9*cnf*$_1$ (E and F), CP9Δ*hlyA*$_1$::*cat*(pKG8) (G and H), and CP9*cnf*$_1$Δ*hlyA*$_1$::*cat* (I and J) for 1 day, and then sections were cut, fixed with formalin, embedded in paraffin, stained with Giemsa stain, and analyzed by light microscopy. Images of a representative sample for each infection are shown at a magnification of ×4 on the left. The rectangles in the images indicate the sections that are shown at a magnification of ×40 on the right. The stars in panels A, C, and G indicate a high degree of edema. The asterisks in panels E and I indicate the luminal space. Note the presence of many inflammatory cells (arrow) in the luminal space in panel B. The arrowheads in panels B and H indicate the intense damage to the urothelium caused by CP9 and CP9Δ*hlyA*$_1$::*cat*(pKG8), respectively. In contrast, the minimal damage caused by CP9Δ*hlyA*$_1$::*cat*, CP9*cnf*$_1$, and CP9*cnf*$_1$Δ*hlyA*$_1$::*cat* is shown in panels D, F, and J, respectively. Panels K and L show a murine bladder instilled with only PBS. U and S in panel L indicate the murine urothelium and submucosa, respectively.

until 48 h, as ascertained by Western blot analysis (Fig. 8B). Moreover, the presence of the CNF1 protein coincided with the presence of CNF1 activity, as measured by a HEp-2 multinucleation assay, up to 48 h after culture inoculation (data not shown). Taken together, these data are consistent with our conclusion based on the results obtained with the murine UTI model that Hly has an impact only early in infection, while CNF1 effects are evident throughout the infection.

Immunofluorescence. To confirm our hematoxylin and eosin and Giemsa stain observations concerning the impact of Hly produced by CP9 on the uroepithelium after 1 day of infection, we treated unstained bladder sections from mice infected with CP9 and the isogenic CP9Δ*hlyA*$_1$::*cat* mutant with antibodies that recognize both the bacteria and the uroplakins, a group of proteins that play a major role in the structure and physiology of the urothelium. We found that at 1 day postinfection, the parental strain had a direct detrimental effect on the structural support indicated by immunoreactivity with antibodies to uroplakins (Fig. 9A). The damage was apparent even in phase-contrast images (Fig. 9C). In contrast, no destructive effect of the CP9Δ*hlyA*$_1$::*cat* mutant on the uroplakin-labeled urothelium was discernible (Fig. 9E and G). Lastly, CP9 seemed to be shed into the lumen of the bladder and did not adhere as well to the damaged uroepithelium (Fig. 9B and D) as the closely uroepithelium-associated mutant CP9Δ*hlyA*$_1$::*cat* (Fig. 9F and H). Taken together, these immunofluorescence results and histological data are suggestive of the significant role that Hly may play in causing uroepithelial tissue damage and even in the location of the bacteria in infected tissue at 1 day postchallenge.

DISCUSSION

In this investigation, we created or used previously generated single, double, or complemented *hlyA*$_1$ or *cnf*$_1$ mutants with the UPEC strain CP9 background. We evaluated the relative impact of expression of CNF1 and Hly on bacterial colonization and histopathology in C3H/HeOuJ mouse bladders and kidneys after intraurethral challenge in a model of ascending UTI. The major findings of this study were as follows. First, we observed no statistically significant impact of either Hly or CNF1 on bacterial colonization in the bladder or kidney in single-mutant infection studies or in a mixed infection with CP9 and CP9Δ*hlyA*$_1$::*cat*. Second, we found that Hly expression by CP9 caused extensive damage to the uroepithelium and augmented tissue hemorrhage in murine bladders at 1 day after challenge. However, no Hly-evoked uroepithelial damage was noted at day 3 or 5 after CP9 challenge. Third, CNF1 was primarily responsible for the striking submucosal edema that was evident in CP9-infected bladders (compared with *cnf*$_1$ mutant-challenged bladders) at days 1 and 3 and to a much lesser extent at day 5 after intraurethral inoculation of

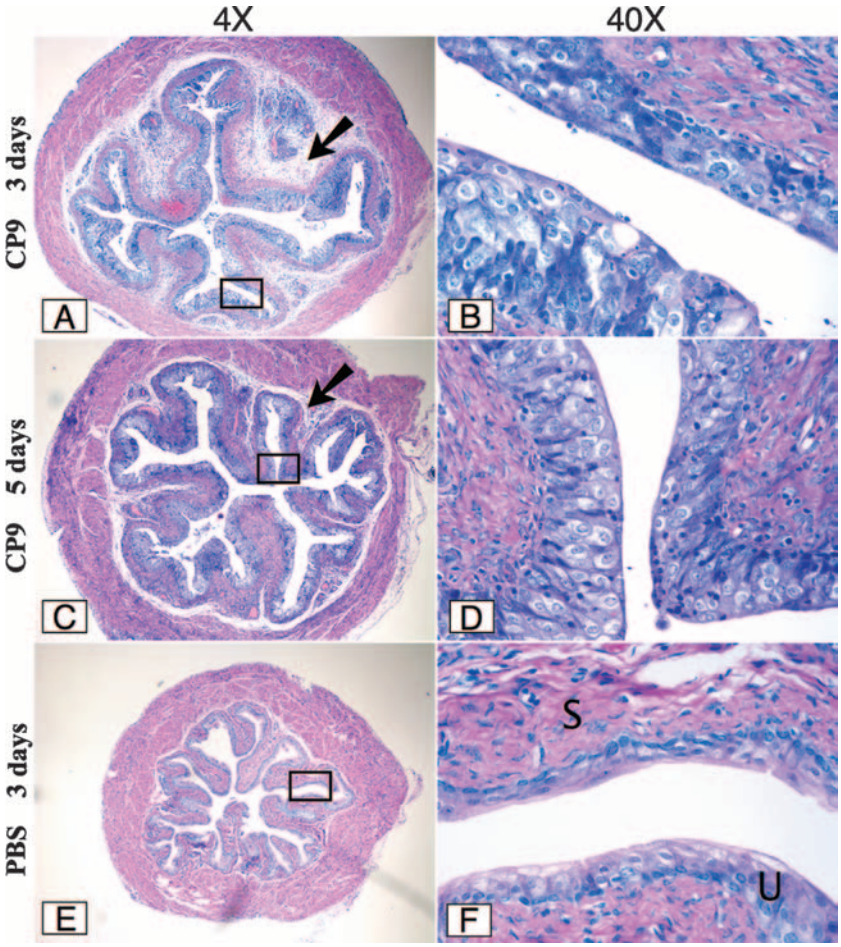

FIG. 7. Infection of female C3H/HeOuJ mice with the CP9 UPEC strain after 3 and 5 days. Groups of five mice were inoculated with CP9, and bladders were harvested after 3 days (A and B) and 5 days (C and D) and then processed as described in the legend to Fig. 6. Images of a representative sample for each infection are shown at a magnification of ×4 on the left. The rectangles in the images indicate the sections that are shown at a magnification of ×40 on the right. Panels E and F show a murine bladder instilled with only PBS and harvested after 3 days. U and S in panel F indicate the murine urothelium and submucosa, respectively. The arrows in panels A and C indicate the degree of interstitial edema at 3 and 5 days, respectively.

bacteria. Fourth, both CNF1 and Hly contributed to leukocyte infiltration into the bladder at day 1 after infection, which was apparent from the lower (albeit not statistically significant) histopathology score obtained with the double mutant.

We concluded that Hly production by strain CP9 had no influence on bacterial colonization of the bladder or kidneys of intraurethrally challenged mice based on the results of both single-strain (CP9 versus CP9Δ*hlyA*$_1$::*cat*) and mixed-strain (CP9 plus CP9Δ*hlyA*$_1$::*cat*) intraurethral infection studies. This conclusion is consistent with several previous reports on the effect of Hly on bacterial persistence at various body sites. Most germane to this study, Haugen and colleagues (30) recently reported that an *hlyA* mutation in wild-type UPEC strain CFT073 (a strain that does not make CNF1) had no effect on colonization of the urinary tract at 48 h after infection. Additionally, Sheshko et al. found that an *hlyA* knockout mutation in an *E. coli* strain used as a probiotic for premature and newborn pigs did not adversely effect colonization of the gut of the animals (60). Lastly, Linggood and Ingram (40) showed that when a mixture of an *E. coli* strain with an Hly-encoding plasmid and an *E. coli* strain without the Hly-encoding plasmid was inoculated intraperitoneally into mice, the nonhemolytic isolate colonized as well as the hemolytic parent strain. Together, our results and those of other workers suggest that any putative (30, 60) or demonstrated (this study) damage evoked by Hly does not translate into enhanced fitness of the infecting *E. coli* strain.

Our observation that colony counts in the urine, bladders, and kidneys of mice 1 day after intraurethral infection with either CP9 or CP9*cnf*$_1$ were not statistically significantly different is consistent with the results of our previous study (55). Nevertheless, in the previous investigation, we did observe an advantage for the wild type in a mixed infection, although no enrichment for CP9 in competition with CP9*cnf*$_1$ was evident in the rat acute prostatitis model (54). Overall, we inferred from these data that CNF1 synthesis provides an edge for persistence of a UPEC strain in the mouse bladder but that the effect is not apparent under the normal circumstances of a UTI (i.e., single-strain infections of an otherwise sterile site [the bladder or the kidney]). Based on our colonization studies with

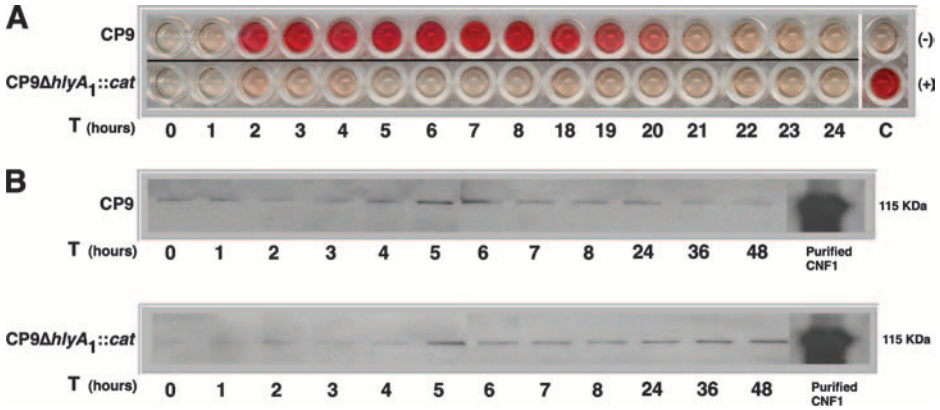

FIG. 8. Alpha-hemolytic activity and CNF1 expression in CP9 strains. Samples were prepared and assays were carried out as described in Material and Methods. (A) Alpha-hemolytic activity of CP9 or CP9Δ*hlyA*$_1$::*cat* supernatants collected hourly from 0 to 48 h was measured by mixing the samples with sheep RBCs. Results for 9 to 17 and 25 to 48 h are not shown. C(−) and C(+) were the negative and positive controls, respectively. (B) Western blot analyses of CP9 and CP9Δ*hlyA*$_1$::*cat* bacterial cell lysates probed with polyclonal anti-CNF1 serum.

the set of CP9 *hlyA*$_1$ and *cnf*$_1$ isogenic mutants, we surmised that other UPEC virulence factors, such as fimbrial and afimbrial adhesins (for a review, see reference 7), are largely responsible for maintenance of UPEC proliferation in organs of the urinary tract.

In striking contrast to the lack of an impact on UPEC colonization, Hly and CNF1 each had a marked, but different, major effect on the histopathology of the bladder (Fig. 5 and 6). Of particular note was the readily apparent destruction of the uroplakin-containing uroepithelium of the bladder mediated by Hly in tissue sections from bladders harvested after 1 day of infection (Fig. 9). The fact that this clear-cut Hly-mediated effect in the bladder had not been previously documented may reflect several unique aspects of this investigation. First, we constructed a mutation in the *hlyA*$_1$ structural gene that is in the *hly* operon linked to *cnf*$_1$ and in the operon (of the two operons in CP9) that we had previously shown was primarily responsible for hemolysis and destruction of bladder cells in vitro (61). Thus, we know that in CP9 the *hly* operon associated with *cnf*$_1$ is more active than the second, unlinked *hly* operon. Second, we used a multicopy plasmid to complement the mutant and restored hemolysis in vitro and damage in vivo. Third, we harvested bladders early in the infection (1 day). Fourth, we viewed cross sections of the entire infected bladder at a magnification of ×4 as a first step in the evaluation of histopathology. This lower-power scan yielded a broader field for examination of all features of acute inflammation.

The fact that we first assessed the entire infected bladder section under low magnification made the extent of CNF1-evoked edema much more apparent. Although we certainly emphasized the impact of CNF1 on acute inflammation in our previous investigations (54, 55), we did not focus on submucosal edema as a prominent feature of the CNF1-augmented immune response. The whole-bladder assessments made us better able to evaluate relative levels of submucosal edema evoked by CP9 on the various days after infection. Thus, we feel comfortable with our conclusion that CNF1 imparts similar degrees of pathology on the bladder at days 1 and 3 after infection and, to a much lesser extent, at day 5. Exactly how CNF1 promotes edema is not clear, but edema may reflect the relationship between the mechanism of action of CNF1 (i.e., constitutive activation of small Rho-GTPases) and the capacity of the toxin to stimulate transcription of cytokine genes involved in acute inflammation (48).

The kinetics of the influence of Hly on the bladder uroepithelium differed from the kinetics of the influence of CNF1 even though the two toxins are reported to be coexpressed in vitro from wild-type UPEC strain J96 (37). Indeed, histological observations revealed only clear Hly-mediated histological damage at 1 day after infection. There are at least four possible explanations for these findings. First, Hly may not be made throughout the course of the infection, a possibility supported by comments of Mobley et al. (46), while CNF1 continues to be synthesized. Second, both Hly and CNF1 may be made only early in infection, but Hly may act quickly (as a membrane-active toxin) and then degrade, while CNF1 may act slowly (as a toxin with an intracellular target) and then remain stable throughout the course of the infection. Third, both Hly and CNF1 may be produced throughout the course of infection, but Hly may be fairly quickly neutralized by preexisting antibodies known to be present in some human sera (18, 59). Fourth, the uroepithelial cells that replace the cells exfoliated during the first 24 h of infection may be resistant to Hly. Our measurements of the kinetics of alpha-hemolytic and CNF1 activities expressed by the wild-type CP9 strain in vitro most strongly support the first explanation. Nevertheless, the actual expression patterns of the toxins in vivo remain to be determined.

In summary, in this report we addressed the relative roles that CNF1 and Hly play in the pathogenesis of UPEC-conferred UTIs. Although in previous reports workers associated Hly production by UPEC strains with pyelonephritis (46, 63, 64), only a few studies focused on the biological and histological impact of this toxin in cystitis. In this investigation, we demonstrated for the first time (to our knowledge) that Hly plays a major role in evoking damage in the uroepithelium and in inducing hemorrhage in the bladder during the early stages of *E. coli*-mediated cystitis in the mouse. We also extended our previous discovery that CNF1 stimulates acute inflammation in

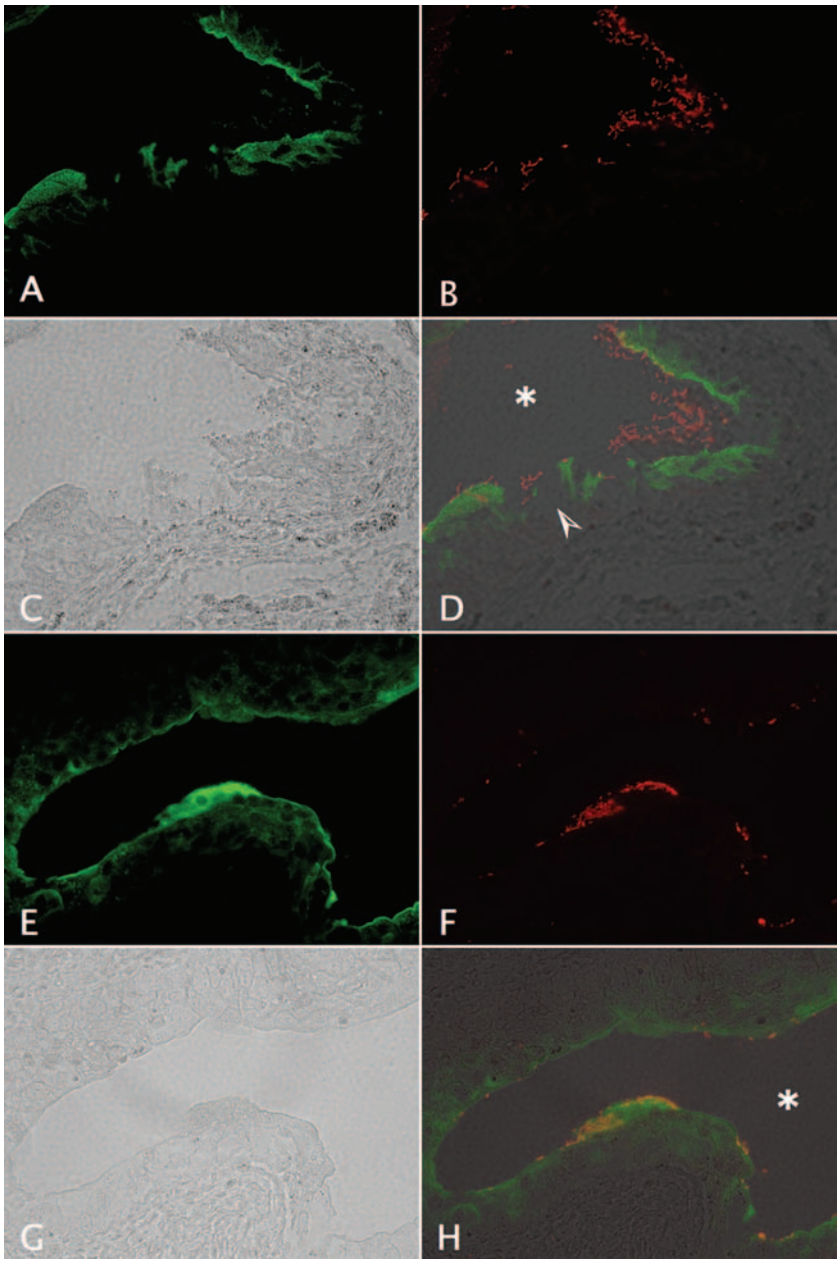

FIG. 9. Impact of CP9 and the isogenic CP9Δ*hlyA*$_1$::*cat* mutant on bladder uroepithelium as revealed by immunostaining of uroplakins. Female C3H/HeOuJ mice were inoculated via the urethra with 2.5×10^7 CFU of CP9 (A to D) or CP9Δ*hlyA*$_1$::*cat* (E to H). Mice were euthanized 1 day later. Bladders were removed, fixed in formalin, embedded in paraffin, processed for immunostaining, and analyzed by immunofluorescence microscopy. The sequence shows samples stained with goat anti-uroplakin III antibody (green) (A and E) and with rabbit anti-*E. coli* antibody (red) (B and F), as well as phase-contrast (C and G) and merged images (D and H). The arrowhead in panel D indicates the severe damage to the uroplakin-lined urothelium caused by CP9, in contrast to the minimal effect on the uroplakin-stained uroepithelium of the CP9Δ*hlyA*$_1$::*cat*-infected bladder in panel H. The asterisks in panels D and H indicate the murine bladder luminal space. Magnification, ×40.

the bladder by revealing the critical function of the toxin in the elicitation of submucosa edema.

ACKNOWLEDGMENTS

We gratefully acknowledge Anastasia L. Sowers for her assistance with the catheterization technique. We thank Farhang Alem, Humberto Carvalho, Steve Darnell, and Dianne McLeod for technical assistance. We are also grateful to Angela Melton-Celsa for assistance with the histology sections and to Cara Olsen for the statistical analysis.

National Institutes of Health grant AI38281 supported this research.

REFERENCES

1. **Aktories, K.** 1997. Rho proteins: targets for bacterial toxins. Trends Microbiol. **5:**282–288.
2. **Alonso, P., J. Blanco, M. Blanco, and E. A. Gonzalez.** 1987. Frequent production of toxins by *Escherichia coli* strains isolated from human urinary tract infections: relation with haemagglutination. FEMS Microbiol. Lett. **48:**391–396.
3. **Andreu, A., A. E. Stapleton, C. Fennell, H. A. Lockman, M. Xercavins, F. Fernandez, and W. E. Stamm.** 1997. Urovirulence determinants in *Escherichia coli* strains causing prostatitis. J. Infect. Dis. **176:**464–469.

4. **Blanco, J., M. P. Alonso, E. A. Gonzalez, M. Blanco, and J. I. Garabal.** 1990. Virulence factors of bacteraemic *Escherichia coli* with particular reference to production of cytotoxic necrotising factor (CNF) by P-fimbriate strains. J. Med. Microbiol. **31:**175–183.
5. **Blanco, J., M. Blanco, M. P. Alonso, J. E. Blanco, E. A. Gonzalez, and J. I. Garabal.** 1992. Characteristics of haemolytic *Escherichia coli* with particular reference to production of cytotoxic necrotizing factor type 1 (CNF1). Res. Microbiol. **143:**869–878.
6. **Blum, G., V. Falbo, A. Caprioli, and J. Hacker.** 1995. Gene clusters encoding the cytotoxic necrotizing factor type 1, Prs-fimbriae and α-hemolysin form the pathogenicity island II of the uropathogenic *Escherichia coli* strain J96. FEMS Microbiol. Lett. **126:**189–195.
7. **Bower, J. M., D. S. Eto, and M. A. Mulvey.** 2005. Covert operations of uropathogenic *Escherichia coli* within the urinary tract. Traffic **6:**18–31.
8. **Caprioli, A., G. Donelli, V. Falbo, R. Possenti, L. G. Roda, G. Roscetti, and F. M. Ruggeri.** 1984. A cell division-active protein from *E. coli*. Biochem. Biophys. Res. Commun. **118:**587–593.
9. **Caprioli, A., V. Falbo, L. G. Roda, F. M. Ruggeri, and C. Zona.** 1983. Partial purification and characterization of an *Escherichia coli* toxic factor that induces morphological cell alterations. Infect. Immun. **39:**1300–1306.
10. **Caprioli, A., V. Falbo, F. M. Ruggeri, L. Baldassarri, R. Bisicchia, G. Ippolito, E. Romoli, and G. Donelli.** 1987. Cytotoxic necrotizing factor production by hemolytic strains of *Escherichia coli* causing extraintestinal infections. J. Clin. Microbiol. **25:**146–149.
11. **Chassin, C., J. M. Goujon, S. Darche, L. du Merle, M. Bens, F. Cluzeaud, C. Werts, E. Ogier-Denis, C. Le Bouguénec, D. Buzoni-Gatel, and A. Vandewalle.** 2006. Renal collecting duct epithelial cells react to pyelonephritis-associated *Escherichia coli* by activating distinct TLR4-dependent and -independent inflammatory pathways. J. Immunol. **177:**4773–4784.
12. **Datsenko, K. A., and B. L. Wanner.** 2000. One-step inactivation of chromosomal genes in *Escherichia coli* K-12 using PCR products. Proc. Natl. Acad. Sci. USA **97:**6640–6645.
13. **Davis, J. M., S. B. Rasmussen, and A. D. O'Brien.** 2005. Cytotoxic necrotizing factor type 1 production by uropathogenic *Escherichia coli* modulates polymorphonuclear leukocyte function. Infect. Immun. **73:**5301–5310.
14. **De Rycke, J., P. Mazars, J. P. Nougayrede, C. Tasca, M. Boury, F. Herault, A. Valette, and E. Oswald.** 1996. Mitotic block and delayed lethality in HeLa epithelial cells exposed to *Escherichia coli* BM2-1 producing cytotoxic necrotizing factor type 1. Infect. Immun. **64:**1694–1705.
15. **De Rycke, J., E. Oswald, and R. Boivin.** 1989. An *in vivo* assay for the detection of cytotoxic strains of *Escherichia coli*. Ann. Rech. Vet. **20:**39–46.
16. **De Rycke, J., L. Phan-Thanh, and S. Bernard.** 1989. Immunochemical identification and biological characterization of cytotoxic necrotizing factor from *Escherichia coli*. J. Clin. Microbiol. **27:**983–988.
17. **Donnenberg, M. S., and R. A. Welch.** 1996. Virulence determinants of uropathogenic *Escherichia coli*, p. 135–174. *In* H. L. T. Mobley and J. W. Warren (ed.), Urinary tract infections: molecular pathogenesis and clinical management. American Society for Microbiology, Washington, DC.
18. **Emödy, L., I. Batai, Jr., M. Kerenyi, J. Szekely, Jr., and L. Polyak.** 1982. Anti-*Escherichia coli* alpha-hemolysin in control and patient sera. Lancet **ii:**986.
19. **Falbo, V., M. Famiglietti, and A. Caprioli.** 1992. Gene block encoding production of cytotoxic necrotizing factor 1 and hemolysin in *Escherichia coli* isolates from extraintestinal infections. Infect. Immun. **60:**2182–2187.
20. **Falbo, V., T. Pace, L. Picci, E. Pizzi, and A. Caprioli.** 1993. Isolation and nucleotide sequence of the gene encoding cytotoxic necrotizing factor 1 of *Escherichia coli*. Infect. Immun. **61:**4909–4914.
21. **Falzano, L., P. Filippini, S. Travaglione, A. G. Miraglia, A. Fabbri, and C. Fiorentini.** 2006. *Escherichia coli* cytotoxic necrotizing factor 1 blocks cell cycle G_2/M transition in uroepithelial cells. Infect. Immun. **74:**3765–3772.
22. **Flatau, G., E. Lemichez, M. Gauthier, P. Chardin, S. Paris, C. Fiorentini, and P. Boquet.** 1997. Toxin-induced activation of the G protein p21 Rho by deamidation of glutamine. Nature **387:**729–733.
23. **Foxman, B., R. Barlow, H. D'Arcy, B. Gillespie, and J. D. Sobel.** 2000. Urinary tract infection: self-reported incidence and associated costs. Ann. Epidemiol. **10:**509–515.
24. **Giamboi-Miraglia, A., S. Travaglione, P. Filippini, A. Fabbri, C. Fiorentini, and L. Falzano.** 2007. A multinucleating *Escherichia coli* cytotoxin perturbs cell cycle in cultured epithelial cells. Toxicol. In Vitro **21:**235–239.
25. **Hacker, J., and J. B. Kaper.** 2000. Pathogenicity islands and the evolution of microbes. Annu. Rev. Microbiol. **54:**641–679.
26. **Hagberg, L., I. Engberg, R. Freter, J. Lam, S. Olling, and C. Svanborg-Edén.** 1983. Ascending, unobstructed urinary tract infection in mice caused by pyelonephritogenic *Escherichia coli* of human origin. Infect. Immun. **40:**273–283.
27. **Hall, A.** 1992. Ras-related GTPases and the cytoskeleton. Mol. Biol. Cell **3:**475–479.
28. **Hall, A.** 1998. Rho GTPases and the actin cytoskeleton. Science **279:**509–514.
29. **Harper, J. R., and T. J. Silhavy.** 2001. Germ warfare: the mechanisms of virulence factor delivery, p. 43–74. *In* E. A. Groisman (ed.), Principles of bacterial pathogenesis. Academic Press, San Diego, CA.
30. **Haugen, B. J., S. Pellett, P. Redford, H. L. Hamilton, P. L. Roesch, and R. A. Welch.** 2007. In vivo gene expression analysis identifies genes required for enhanced colonization of the mouse urinary tract by uropathogenic *Escherichia coli* strain CFT073 *dsdA*. Infect. Immun. **75:**278–289.
31. **Johnson, J. R.** 1991. Virulence factors in *Escherichia coli* urinary tract infection. Clin. Microbiol. Rev. **4:**80–128.
32. **Johnson, J. R., and J. J. Brown.** 1996. Defining inoculation conditions for the mouse model of ascending urinary tract infection that avoid immediate vesicoureteral reflux yet produce renal and bladder infection. J. Infect. Dis. **173:**746–749.
33. **Johnson, J. R., T. A. Russo, F. Scheutz, J. J. Brown, L. Zhang, K. Palin, C. Rode, C. Bloch, C. F. Marrs, and B. Foxman.** 1997. Discovery of disseminated J96-like strains of uropathogenic *Escherichia coli* O4:H5 containing genes for both PapG(J96) (class I) and PrsG(J96) (class III) Gal(alpha1-4)Gal-binding adhesins. J. Infect. Dis. **175:**983–988.
34. **Koronakis, V., J. Eswaran, and C. Hughes.** 2003. The type I export mechanism, p. 71–79. *In* D. L. Burns, J. T. Barbieri, B. H. Iglewski, and R. Rappuoli (ed.), Bacterial protein toxins. ASM Press, Washington, DC.
35. **Lally, E. T., R. B. Hill, I. R. Kieba, and J. Korostoff.** 1999. The interaction between RTX toxins and target cells. Trends Microbiol. **7:**356–361.
36. **Landraud, L., M. Gauthier, T. Fosse, and P. Boquet.** 2000. Frequency of *Escherichia coli* strains producing the cytotoxic necrotizing factor (CNF1) in nosocomial urinary tract infections. Lett. Appl. Microbiol. **30:**213–216.
37. **Landraud, L., M. Gibert, M. R. Popoff, P. Boquet, and M. Gauthier.** 2003. Expression of *cnf1* by *Escherichia coli* J96 involves a large upstream DNA region including the *hlyCABD* operon, and is regulated by the RfaH protein. Mol. Microbiol. **47:**1653–1667.
38. **Lerm, M., G. Schmidt, U. M. Goehring, J. Schirmer, and K. Aktories.** 1999. Identification of the region of Rho involved in substrate recognition by *Escherichia coli* cytotoxic necrotizing factor 1 (CNF1). J. Biol. Chem. **274:**28999–29004.
39. **Lerm, M., J. Selzer, A. Hoffmeyer, U. R. Rapp, K. Aktories, and G. Schmidt.** 1999. Deamidation of Cdc42 and Rac by *Escherichia coli* cytotoxic necrotizing factor 1: activation of c-Jun N-terminal kinase in HeLa cells. Infect. Immun. **67:**496–503.
40. **Linggood, M. A., and P. L. Ingram.** 1982. The role of alpha haemolysin in the virulence of *Escherichia coli* for mice. J. Med. Microbiol. **15:**23–30.
41. **Martinez, J. J., and S. J. Hultgren.** 2002. Requirement of Rho-family GTPases in the invasion of type 1-piliated uropathogenic *Escherichia coli*. Cell. Microbiol. **4:**19–28.
42. **Martinez, J. J., M. A. Mulvey, J. D. Schilling, J. S. Pinkner, and S. J. Hultgren.** 2000. Type 1 pilus-mediated bacterial invasion of bladder epithelial cells. EMBO J. **19:**2803–2812.
43. **Meysick, K. C., M. Mills, and A. D. O'Brien.** 2001. Epitope mapping of monoclonal antibodies capable of neutralizing cytotoxic necrotizing factor type 1 of uropathogenic *Escherichia coli*. Infect. Immun. **69:**2066–2074.
44. **Mills, M., K. C. Meysick, and A. D. O'Brien.** 2000. Cytotoxic necrotizing factor type 1 of uropathogenic *Escherichia coli* kills cultured human uroepithelial 5637 cells by an apoptotic mechanism. Infect. Immun. **68:**5869–5880.
45. **Mitsumori, K., A. Terai, S. Yamamoto, S. Ishitoya, and O. Yoshida.** 1999. Virulence characteristics of *Escherichia coli* in acute bacterial prostatitis. J. Infect. Dis. **180:**1378–1381.
46. **Mobley, H. L., D. M. Green, A. L. Trifillis, D. E. Johnson, G. R. Chippendale, C. V. Lockatell, B. D. Jones, and J. W. Warren.** 1990. Pyelonephritogenic *Escherichia coli* and killing of cultured human renal proximal tubular epithelial cells: role of hemolysin in some strains. Infect. Immun. **58:**1281–1289.
47. **Mulvey, M. A., Y. S. Lopez-Boado, C. L. Wilson, R. Roth, W. C. Parks, J. Heuser, and S. J. Hultgren.** 1998. Induction and evasion of host defenses by type 1-piliated uropathogenic *Escherichia coli*. Science **282:**1494–1497.
48. **Munro, P., G. Flatau, A. Doye, L. Boyer, O. Oregioni, J. L. Mege, L. Landraud, and E. Lemichez.** 2004. Activation and proteasomal degradation of Rho GTPases by cytotoxic necrotizing factor-1 elicit a controlled inflammatory response. J. Biol. Chem. **279:**35849–35857.
49. **National Institutes of Health.** 1985. Guide for the care and use of laboratory animals. National Institutes of Health publication no. 85-23. National Institutes of Health, Bethesda, MD.
50. **Nobes, C. D., and A. Hall.** 1995. Rho, Rac, and Cdc42 GTPases regulate the assembly of multimolecular focal complexes associated with actin stress fibers, lamellipodia, and filopodia. Cell **81:**53–62.
51. **Real, J. M., P. Munro, C. Buisson-Touati, E. Lemichez, P. Boquet, and L. Landraud.** 2007. Specificity of immunomodulator secretion in urinary samples in response to infection by alpha-hemolysin and CNF1 bearing uropathogenic *Escherichia coli*. Cytokine **37:**22–25.
52. **Ridley, A. J., and A. Hall.** 1992. The small GTP-binding protein Rho regulates the assembly of focal adhesions and actin stress fibers in response to growth factors. Cell **70:**389–399.
53. **Ridley, A. J., H. F. Paterson, C. L. Johnston, D. Diekmann, and A. Hall.** 1992. The small GTP-binding protein Rac regulates growth factor-induced membrane ruffling. Cell **70:**401–410.
54. **Rippere-Lampe, K. E., M. Lang, H. Ceri, M. Olson, H. A. Lockman, and A. D. O'Brien.** 2001. Cytotoxic necrotizing factor type 1-positive *Escherichia*

coli causes increased inflammation and tissue damage to the prostate in a rat prostatitis model. Infect. Immun. **69:**6515–6519.
55. **Rippere-Lampe, K. E., A. D. O'Brien, R. Conran, and H. A. Lockman.** 2001. Mutation of the gene encoding cytotoxic necrotizing factor type 1 (*cnf1*) attenuates the virulence of uropathogenic *Escherichia coli*. Infect. Immun. **69:**3954–3964.
56. **Russo, T. A., J. E. Guenther, S. Wenderoth, and M. M. Frank.** 1993. Generation of isogenic K54 capsule-deficient *Escherichia coli* strains through TnphoA-mediated gene disruption. Mol. Microbiol. **9:**357–364.
57. **Schmidt, G., P. Sehr, M. Wilm, J. Selzer, M. Mann, and K. Aktories.** 1997. Gln 63 of Rho is deamidated by *Escherichia coli* cytotoxic necrotizing factor-1. Nature **387:**725–729.
58. **Schmidt, H., and M. Hensel.** 2004. Pathogenicity islands in bacterial pathogenesis. Clin. Microbiol. Rev. **17:**14–56.
59. **Seetharama, S., S. J. Cavalieri, and I. S. Snyder.** 1988. Immune response to *Escherichia coli* alpha-hemolysin in patients. J. Clin. Microbiol. **26:** 850–856.
60. **Sheshko, V., J. Hejnova, Z. Rehakova, J. Sinkora, M. Faldyna, P. Alexa, J. Felsberg, R. Nemcova, A. Bomba, and P. Sebo.** 2006. HlyA knock out yields a safer *Escherichia coli* A0 34/86 variant with unaffected colonization capacity in piglets. FEMS Immunol. Med. Microbiol. **48:**257–266.
61. **Smith, Y. C., K. K. Grande, S. B. Rasmussen, and A. D. O'Brien.** 2006. Novel three-dimensional organoid model for evaluation of the interaction of uropathogenic *Escherichia coli* with terminally differentiated human urothelial cells. Infect. Immun. **74:**750–757.
62. **Swenson, D. L., N. O. Bukanov, D. E. Berg, and R. A. Welch.** 1996. Two pathogenicity islands in uropathogenic *Escherichia coli* J96: cosmid cloning and sample sequencing. Infect. Immun. **64:**3736–3743.
63. **Waalwijk, C., D. M. MacLaren, and J. de Graaff.** 1983. In vivo function of hemolysin in the nephropathogenicity of *Escherichia coli*. Infect. Immun. **42:**245–249.
64. **Warren, J. W., H. L. Mobley, J. R. Hebel, and A. L. Trifillis.** 1995. Cytolethality of hemolytic *Escherichia coli* to primary human renal proximal tubular cell cultures obtained from different donors. Urology **45:**706–710.
65. **Welch, R. A.** 1991. Pore-forming cytolysins of gram-negative bacteria. Mol. Microbiol. **5:**521–528.
66. **Yamamoto, S., T. Tsukamoto, A. Terai, H. Kurazono, Y. Takeda, and O. Yoshida.** 1995. Distribution of virulence factors in *Escherichia coli* isolated from urine of cystitis patients. Microbiol. Immunol. **39:**401–404.

Editor: V. J. DiRita